Supporting Information for "Seismic diffraction imaging to characterise mass-transport complexes: examples from the Gulf of Cadiz, south west Iberian Margin"

Jonathan Ford[1,2], Roger Urgeles[3], Angelo Camerlenghi[1], Eulàlia Gràcia[3]

[1]National Institute of Oceanography and Applied Geophysics - OGS

[2]Dipartimento di Matematica e Geoscienze, Università di Trieste

[3]Institut de Ciències del Mar, CSIC

Contents of this file

Corresponding author: J. Ford (jford@inogs.it)

Text S1: Introduction

This supporting information file contains figures, tables and datasets to supplement the main manuscript. Input data to the conventional and diffraction imaging workflows, including broadband pre-processed pre-stack gathers (SEG-Y format) and horizons used in processing are archived and available in Ford (2020). These data were acquired and processed onboard as part of the INSIGHT project, comprising two research cruises in May 2018 and October 2019 (Gràcia et al., 2018; Urgeles et al., 2019).

Text S2: Interpretation of MTC A extent and thickness

In the main text we include a thickness map of MTC A, a mass-transport complex (MTC) intersected by profile INS2-Line1 (Fig. 10). The thickness of the MTC was derived from a combination of multi-beam swatch bathymetry, sub-bottom profiler and multi-channel seismic data (Fig. S4).

The lateral extent (bounding polygon) of the MTC was interpeted using the bathymetry and sub-bottom profiler data. The basal surface of the MTC was interpreted using the multi-channel seismic profiles (Figs. S1 and S2) as the sub-bottom profiler data lacked the penetration to consistently image the basal reflector. An example of the sub-bottom profile data is shown in Fig. S3. The top surface of the MTC was assumed to be equivalent to the seafloor.

The basal surface grid was estimated by gridding the picked basal surface horizon with a constraint that the thickness at the bounding polygon was zero. The thickness map was then calculated as the difference between the top surface (bathymetry) and the gridded basal surface.

References

Ford, J. (2020). *Multi-channel seismic reflection profiles MP06b and INS-Line1 (INSIGHT cruises).* Zenodo. (Dataset) doi: 10.5281/zenodo.3946170

Gràcia, E., Urgeles, R., Rothenbeck, M., Wenzlaff, E., Steinführer, A., Kurbjuhn, T., ... INSIGHT Leg 1 cruise party (2018). *ImagiNg large SeismogenIc and tsunamiGenic structures of the Gulf of Cadiz with ultra-High resolution Technologies (INSIGHT) Leg 1 survey cruise report* (Tech. Rep.). Institut de Ciències del Mar - CSIC.

Urgeles, R., INSIGHT Leg 2 cruise shipboard participants, et al. (2019). *ImagiNg large SeismogenIc and tsunamiGenic structures of the Gulf of Cadiz with ultra-High resolution Technologies (INSIGHT) Leg 2 survey cruise report* (Tech. Rep.). Institute of Marine Sciences, Barcelona.

Vakulenko, S. A., Buryak, S. V., Gofman, P. A., & Finikov, D. B. (2014). Deghosting of High Resolution Marine Seismic Data by Adaptive Filtering Algorithm. In (Vol. 2014, pp. 1–5). European Association of Geoscientists & Engineers. doi: 10.3997/2214-4609.20142133

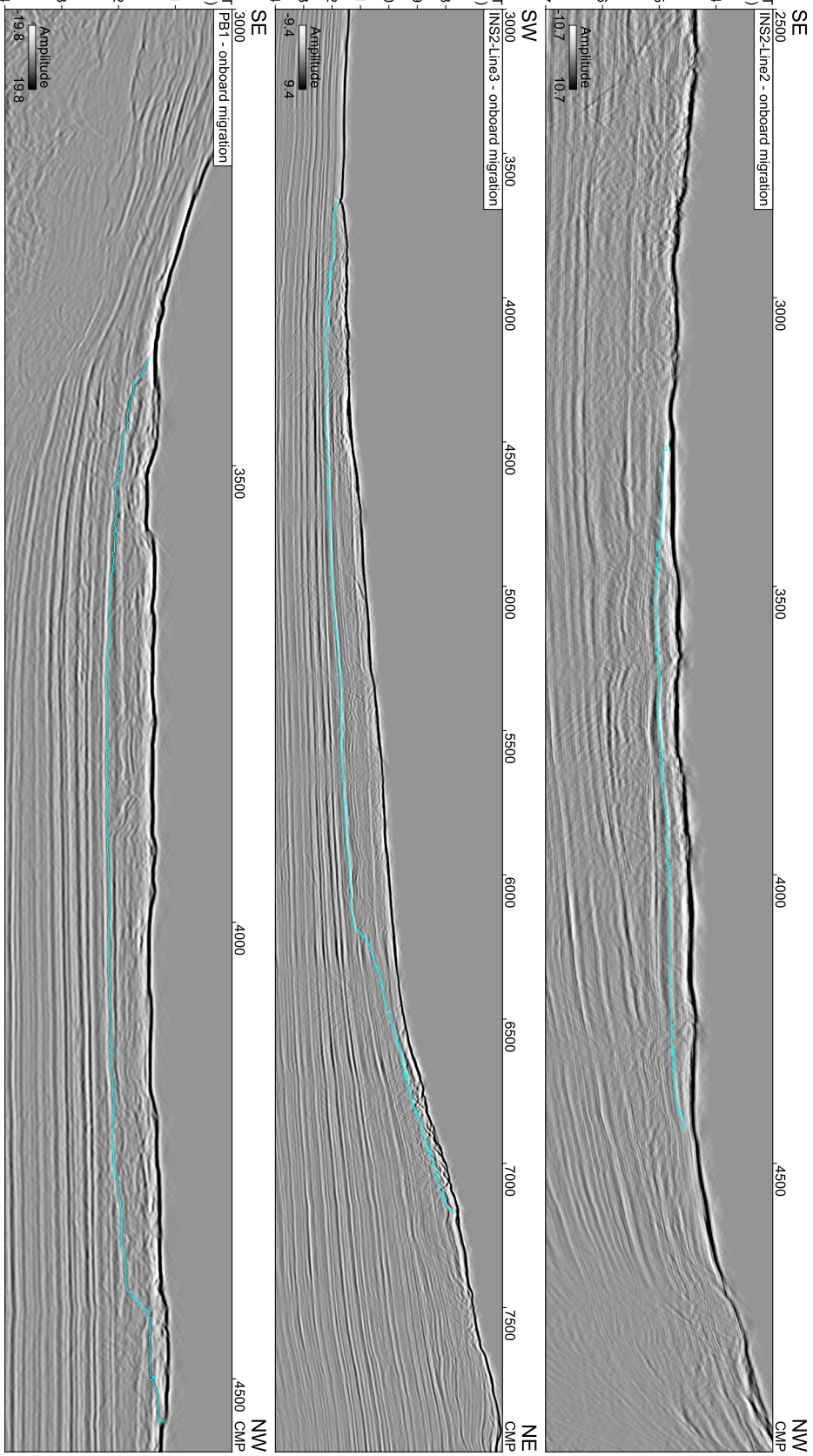

Figure S1. Multi-channel seismic profiles with the interpreted basal surface of MTC A shown in blue. a) INS2-Line2. b) INS2-Line3. c) PB1.

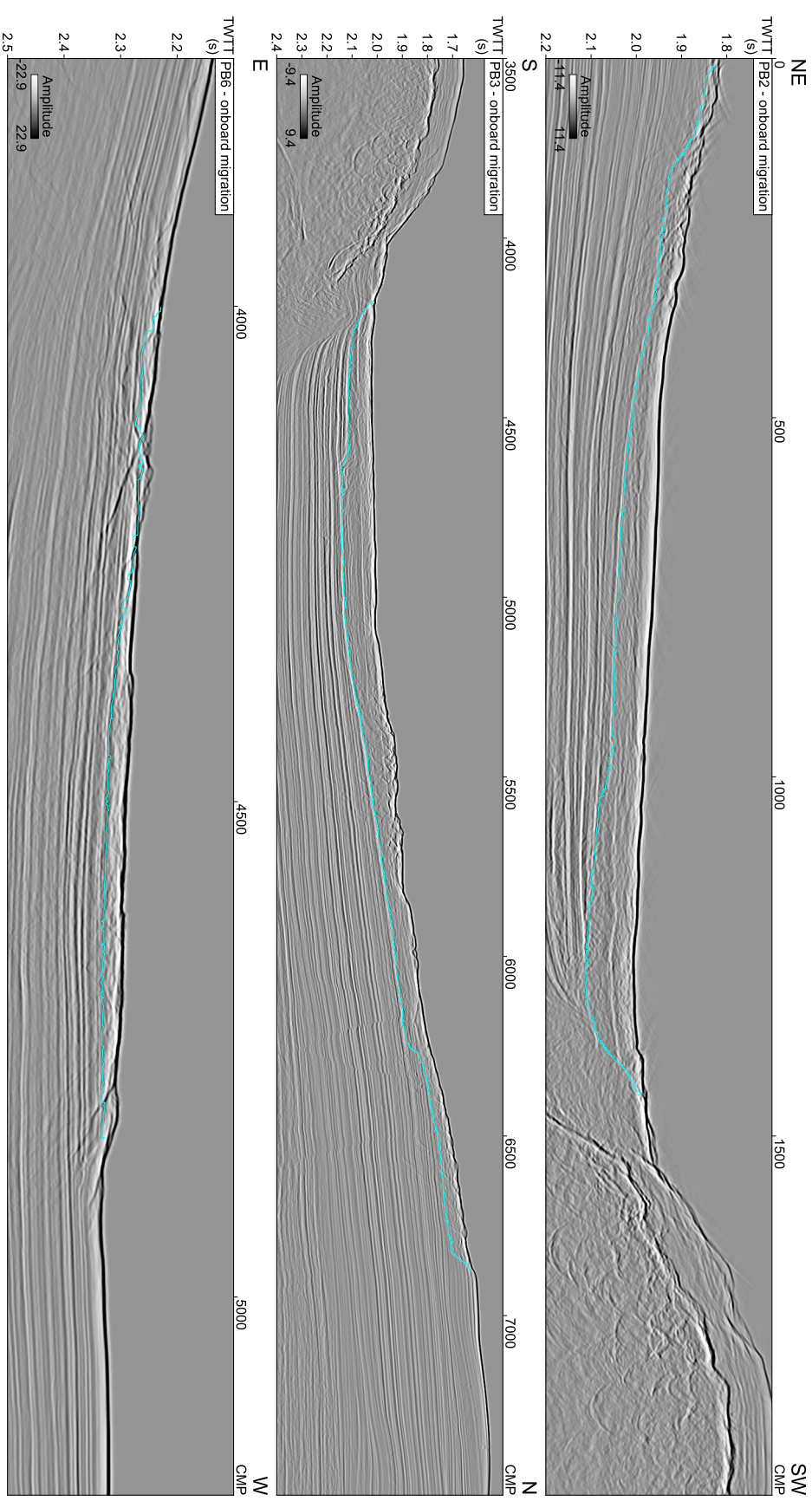

Figure S2. Multi-channel seismic profiles with the interpreted basal surface of MTC A shown in blue. a) PB2. b) PB3. c) PB6.

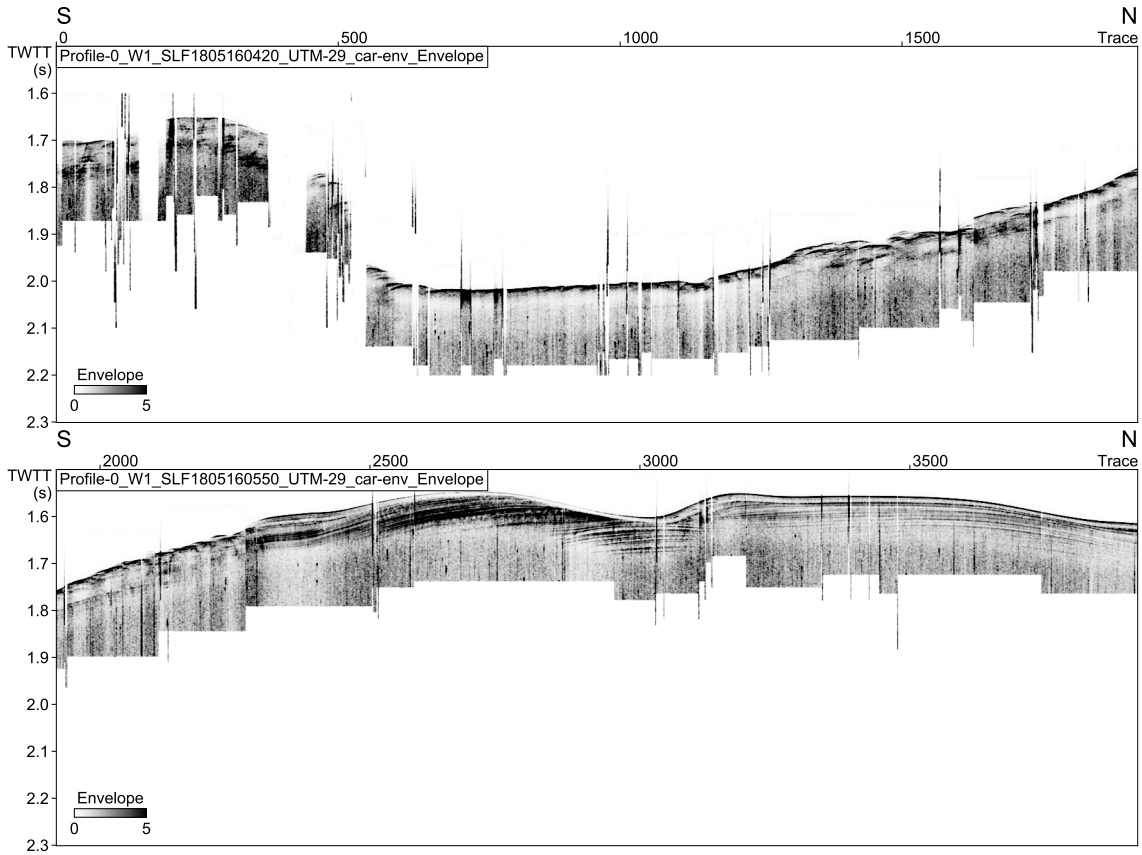

Figure S3. Example of a sub-bottom profile across the MTC.

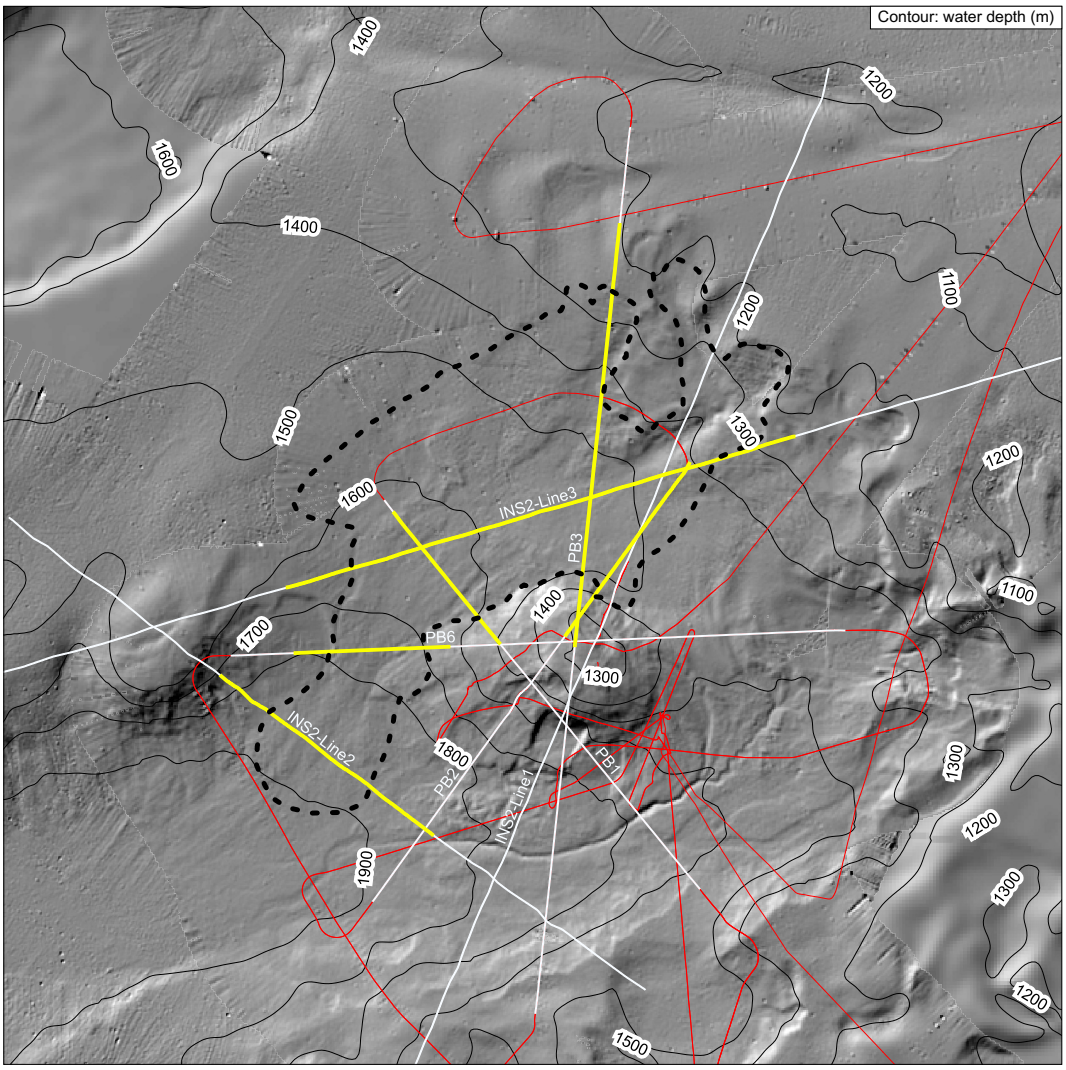

Figure S4. Map of data used to derive thickness of MTC A. (white) Multi-channel seismic profiles. (red) Sub-bottom profiles. (Dashed black) Interpreted outline of MTC A based on sub-bottom profiles and bathymetry.

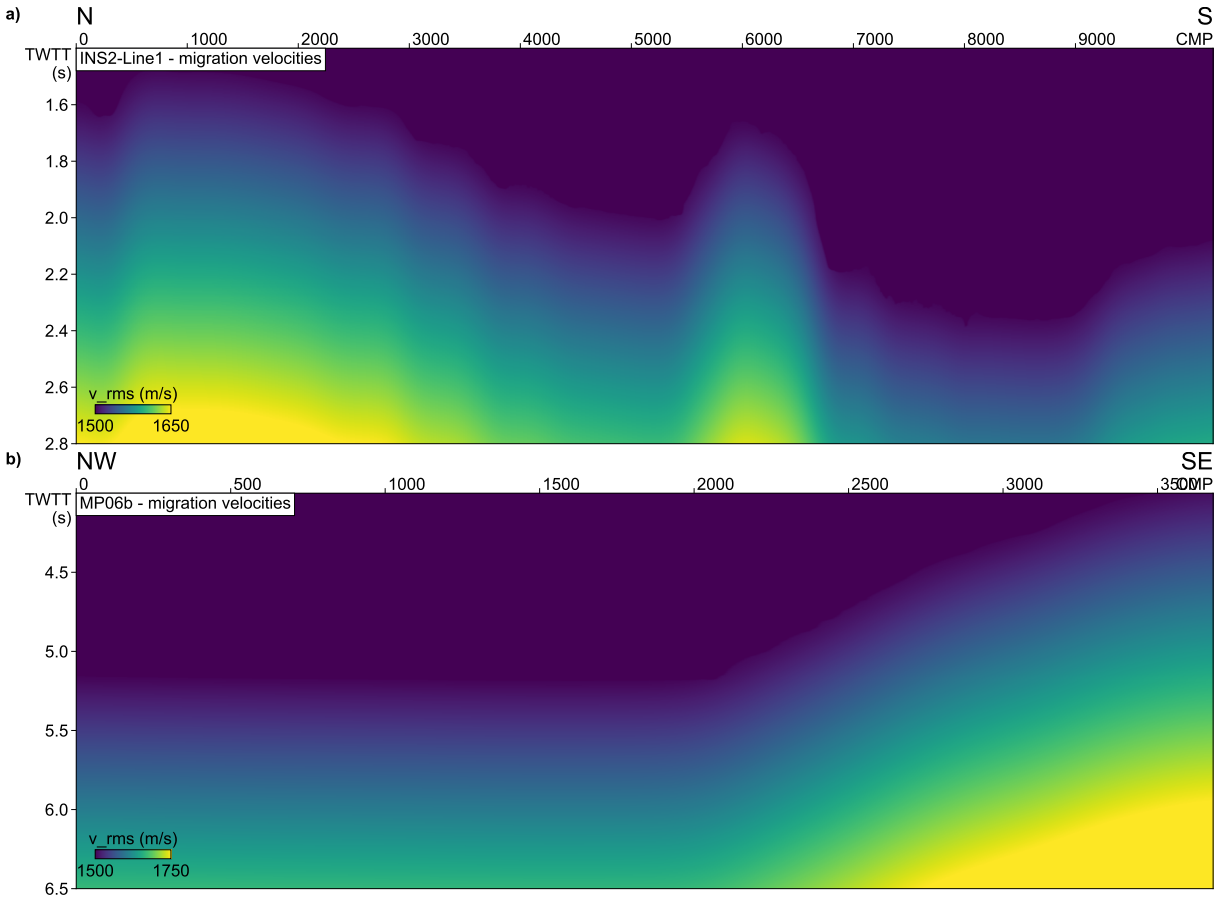

Figure S5. Migration velocities used in the main manuscript for seismic profiles a) INS2-Line1 and b) MP06b. The sediment velocity gradients were derived during onboard processing by migrating with a range of gradients and comparing the overall image quality for a a range of profiles in each area (Gràcia et al., 2018; Urgeles et al., 2019). SEG-Y versions and waterbottom horizons are available in Ford (2020).

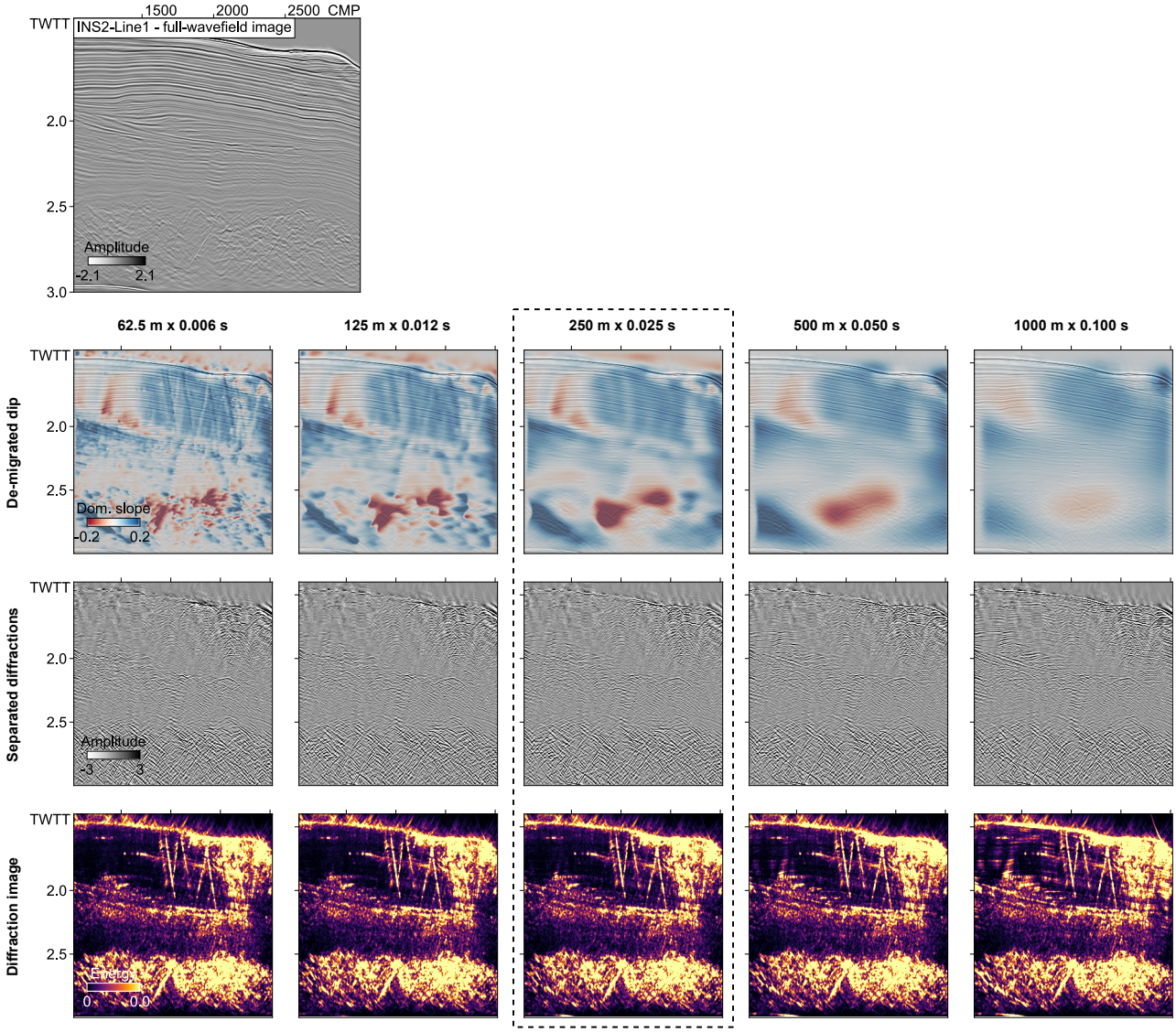

Figure S6. Dip sensitivity tests for a portion of INS2-Line1. Above: the full-wavefield image of a section of the profile. Below: un-migrated full-wavefield stack with de-migrated dip field (dominant slope) overlay, resulting separated diffraction stack, resulting migrated diffraction image. Left-to-right: increasing smoothing window for dip field. The smoothing window used in the main manuscript for INS2-Line1 is highlighted.

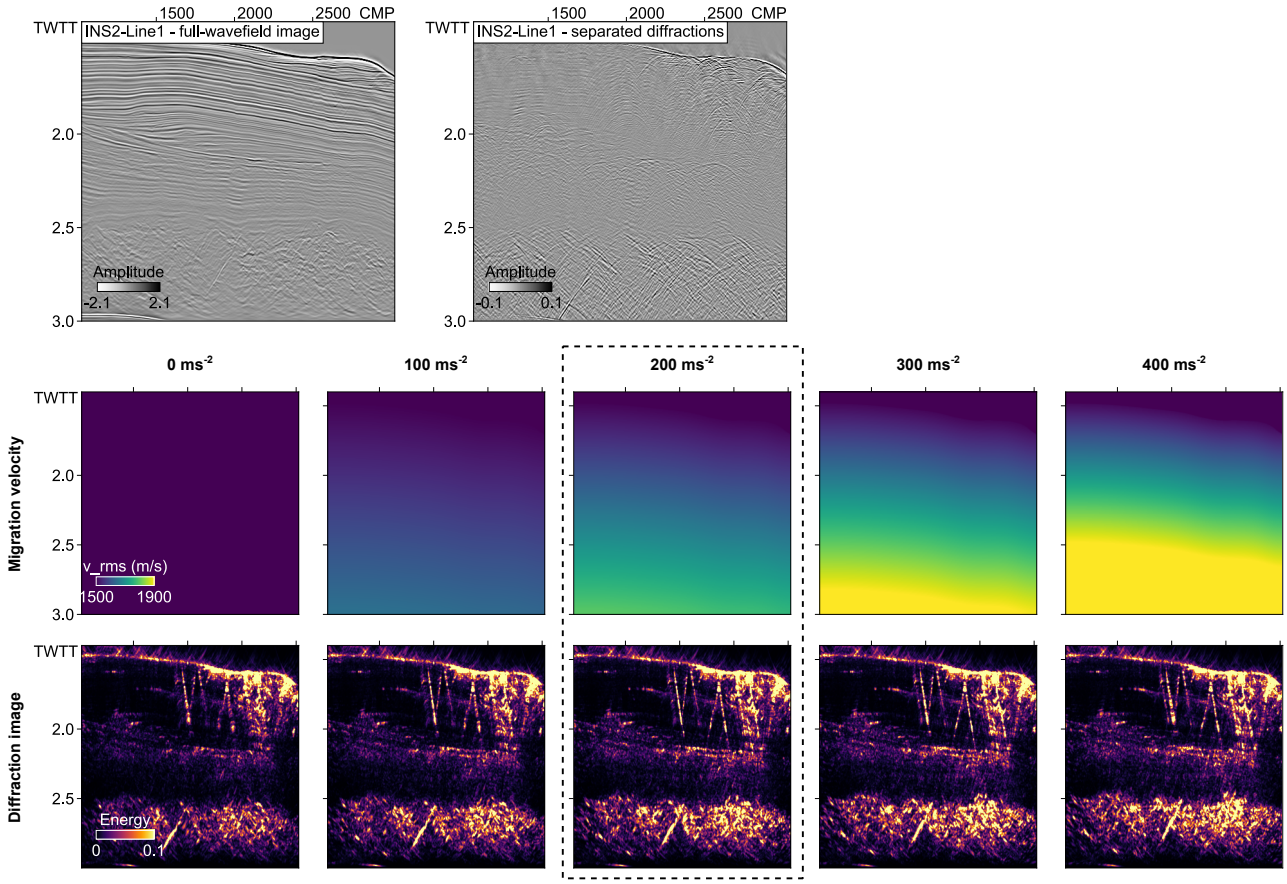

Figure S7. Migration velocity sensitivity tests for a portion of INS2-Line1. Above: (left) the full-wavefield image of a section of the profile, (right) the unmigrated separated diffractions. Below: migration velocity field, resulting migrated diffraction image. Left-to-right: increasing migration velocity. The migration velocity used in the main manuscript for INS2-Line1 is highlighted.

Table S1. Acquisition parameters for multi-channel seismic profiles MP06b and INS2-Line1.

	Seismic profile	
	MP06b	INS2-Line1
Vessel	B/O Sarmiento de Gamboa	
Acquisition date	May 2018	October 2019
Profile length	11.6 km	32.2 km
Seismic source	Airgun array (10 × G-Gun II, 930 cu. in. total volume)	
Source depth	3.5 m	
Shot interval	18.5 m	12.5 m
Recording array	Solid-state digital streamer (GeoEel Geometrics)	
Receiver groups	72	56
Receiver group interval	6.25 m	
Streamer depth	3.5 m	
Near offset	104.9 m	
Far offset	548.75 m	448.65 m
Record length	8.0 s	5.8 s
Acquisition sample interval	0.5 ms	
Nominal coverage	12-fold	14-fold

Table S2. Outline of the broadband pre-processing flow for multi-channel seismic profiles MP06b and INS2-Line1

Resample to 1 ms (anti-alias filter: 380–450 Hz high cut)
Remove recording delay (50 ms)
Navigation and geometry import
Trace editing (drop bad shots)
Swell noise attenuation (2–4 Hz low-cut filter, time-frequency trim in shot domain (2–40 Hz) and channel domain (2–20 Hz))
Source and receiver ghost removal (SharpSeis de-ghost; Vakulenko et al., 2014)
Designature (de-bubble filter and zero-phase correction, operator derived by stacking waterbottom reflection)
Shot domain $\tau - p$ mute (passing range $-200 < p < 400$ µs m^{-1})
CMP binning (3.125 m interval)